

See discussions, stats, and author profiles for this publication at: <https://www.researchgate.net/publication/7138217>

# Continuous Flow Analytical Microsystems Based on Low-Temperature Co-Fired Ceramic Technology. Integrated Potentiometric Detection Based on Solvent Polymeric Ion-Selective Electrode...

ARTICLE in ANALYTICAL CHEMISTRY · JUNE 2006

Impact Factor: 5.64 · DOI: 10.1021/ac051994k · Source: PubMed

---

CITATIONS

33

---

READS

33

6 AUTHORS, INCLUDING:



**Manel Bautista**

Novartis

13 PUBLICATIONS 274 CITATIONS

SEE PROFILE



**Antonio C. Seabra**

University of São Paulo

35 PUBLICATIONS 186 CITATIONS

SEE PROFILE



**Mario Ricardo Gongora Rubio**

Instituto de Pesquisas Tecnológicas

39 PUBLICATIONS 408 CITATIONS

SEE PROFILE



**Julián Alonso-Chamarro**

Autonomous University of Barcelona

161 PUBLICATIONS 1,864 CITATIONS

SEE PROFILE

# Continuous Flow Analytical Microsystems Based on Low-Temperature Co-Fired Ceramic Technology. Integrated Potentiometric Detection Based on Solvent Polymeric Ion-Selective Electrodes

Nuria Ibanez-Garcia,<sup>†</sup> Manel Bautista Mercader,<sup>†</sup> Zaira Mendes da Rocha,<sup>‡</sup> Carlos Antonio Seabra,<sup>‡</sup> Mário Ricardo Góngora-Rubio,<sup>‡,§</sup> and Julián Alonso Chamarro<sup>\*,†</sup>

Grup de Sensors i Biosensors, Departament de Química Analítica, Edifici C, Universitat Autònoma de Barcelona, 08193 Cerdanyola del Vallès, Barcelona, Spain, Laboratório de Sistemas Integráveis (LSI), Universidade de São Paulo, C. Universitaria CEP 05508, São Paulo, Brazil, and Instituto de Pesquisas Tecnológicas (IPT), Av. Prof. Almeida Proda 532 C. Universitaria CEP 05508, São Paulo, Brazil

In this paper, the low-temperature co-fired ceramics (LTCC) technology, which has been commonly used for electronic applications, is presented as a useful alternative to construct continuous flow analytical microsystems. This technology enables not only the fabrication of complex three-dimensional structures rapidly and at a realistic cost but also the integration of the elements needed to carry out a whole analytical process, such as pretreatment steps, mixers, and detection systems. In this work, a simple and general procedure for the integration of ion-selective electrodes based on liquid ion exchanger is proposed and illustrated by using ammonium- and nitrate-selective membranes. Additionally, a screen-printed reference electrode was easily incorporated into the microfluidic LTCC structure allowing a complete on-chip integration of the potentiometric detection. Analytical features of the proposed systems are presented.

Over the past decade, advances in the miniaturization field, especially those related to microfluidics, have been intensively applied to the development of analytical instrumentation in order to solve chemical and biological problems. The (bio)analytical chemistry field has become one of the most important users of the scaling technologies due to their inherent advantages, such as low cost (mass production), reduction of sample and reagents consumption, higher analysis frequency, compact design, ease of operation, and portability.

Ever since the 1990s, the combination of the miniaturization–integration concepts has helped to establish the conceptual bases to develop a new generation of analytical instrumentation, the so-called micro total analysis systems ( $\mu$ TAS).<sup>1</sup> These  $\mu$ TAS are made

up of miniaturized devices able to integrate the whole analytical process.<sup>2–5</sup> The fusion of the microelectronic technologies with the continuous flow methodological concepts, widely applied in analytical chemistry, provides the tools needed to obtain this kind of analytical instrumentation. Unfortunately, the high variety of key components needed to design  $\mu$ TAS has delayed the attainment of the considered goals. Among the functional elements needed to give solution to the widest range of analytical problems, some of the most remarkable are microfluidic structures, as well as their connections,<sup>6</sup> pumps<sup>7–9</sup> and valves,<sup>10,11</sup> injection elements,<sup>12,13</sup> reactors,<sup>14–16</sup> filters,<sup>17</sup> separation and preconcentration devices,<sup>18</sup> and microsensors (physical and chemical).<sup>19–21</sup>

- (2) Reyes, D. R.; Iossifidis, D.; Auroux, P. A.; Manz, A. *Anal. Chem.* **2002**, *74*, 2623–2636.
- (3) Auroux, P. A.; Iossifidis, D.; Reyes, D. R.; Manz, A. *Anal. Chem.* **2002**, *74*, 2637–2652.
- (4) Ng, J. M. K.; Gitlin, I.; Stroock, A. D.; Whitesides, G. M. *Electrophoresis* **2002**, *23*, 3461–3473.
- (5) Vilkner, T.; Janasek, D.; Manz, A. *Anal. Chem.* **2004**, *76*, 3373–3386.
- (6) Gonzalez, C.; Collins, S. D.; Smith, R. L. *Sens. Actuators, B: Chem.* **1998**, *49*, 40–45.
- (7) Santra, S.; Holloway, P.; Batich, C. D. *Sens. Actuators, B: Chem.* **2002**, *87*, 358–364.
- (8) Hatch, A.; Kamholz, A. E.; Holman, G.; Yager, P.; Bohringer, K. F. J. *Microelectromech. Syst.* **2001**, *10*, 215–221.
- (9) Nguyen, N. T.; Huang, X. Y. *Sens. Actuators, B: Phys.* **2001**, *88*, 104–111.
- (10) Ohori, T.; Shoji, S.; Miura, K.; Yotsumoto, A. *Sens. Actuators, B: Phys.* **1998**, *64*, 57–62.
- (11) Jeon, N. L.; Chiu, D. T.; Wargo, C. J.; Wu, H. K.; Choi, I. S.; Anderson, J. R.; Whitesides, G. M., *Biomed. Microdevices* **2002**, *4*, 117–121.
- (12) Zhang, C. X.; Manz, A. *Anal. Chem.* **2001**, *73*, 2656–2662.
- (13) Greenway, G. M.; Haswell, S. J.; Petsul, P. H. *Anal. Chim. Acta* **1999**, *387*, 1–10.
- (14) Greenwood, P. A.; Greenway, G. M. *TrAC—Trends Anal. Chem.*, **2002**, *21*, 726–740.
- (15) Bertsch, A.; Heimgartner, S.; Cousseau, P.; Renaud, P. *Lab Chip* **2001**, *1*, 56–60.
- (16) Woolley, A. T.; Hadley, D.; Landre, P.; de Mello, A. J.; Mathies, R. A.; Northrup, M. A. *Anal. Chem.* **1996**, *68*, 4081–4086.
- (17) Andersson, H.; van der Wijngaart, W.; Enoksson, P.; Stemme, G. *Sens. Actuators, B: Chem.* **2000**, *67*, 203–208.
- (18) Fintschenko, Y.; van den Berg, A. J. *Chromatogr., A* **1998**, *819*, 3–12.
- (19) Schwarz, M. A.; Hauser, P. C. *Lab Chip* **2001**, *1*, 1–6.
- (20) Wang, J. *TrAC—Trends Anal. Chem.* **2002**, *21*, 226–232.

\* Corresponding author. E-mail: julian.alonso@uab.es. Tel.: +34935811836. Fax: +34935812379.

<sup>†</sup> Universitat Autònoma de Barcelona.

<sup>‡</sup> Universidade de São Paulo.

<sup>§</sup> Instituto de Pesquisas Tecnológicas (IPT).

(1) Manz, A.; Graber, N.; Widmer, H. M. *Sens. Actuators, B: Chem.* **1990**, *1*, 244–248.

Great advances have already been done in the microfluidics and detection field; however, there is still plenty of work in the area of fluids handling systems (involving microactuators such as pumps, valves, and switches). Additionally, other problems dealing with packaging,<sup>22–25</sup> as well as with the interface with its environment and other mesoscale devices and 3-D structures implementation are still partially unsolved.

Nevertheless, some hybrid TAS have already been constructed. Although not each of their elements was miniaturized, one can notice the main advantages of the miniaturization–integration binomial.

Glass and silicon have been the most widely used materials with miniaturization purposes; this is in part due to their versatility and chemical resistivity, the relatively straightforward fabrication, and the easy integration of optical detection. On the other hand, plastic devices have a number of advantages over glass and silicon technology, which include the speed of manufacture and lower fabrication cost.<sup>26</sup> Several techniques have been used to construct microfluidic systems using polymers. Thus, we find methodologies such as imprinting and hot embossing,<sup>27</sup> soft lithography,<sup>28,29</sup> or X-ray lithography.<sup>30</sup>

However, as has been mentioned before, most of these methods require postfabrication sealing of the microchannels to form an enclosed structure. Sealing of polymer-made microchannels is generally much simpler than with silicon or glass channels and can often be accomplished using low-temperature thermal annealing; this is the case of elastomeric polymers, such as PDMS,<sup>24</sup> which have excellent adhesion to a wide variety of substrate materials and can be used to enclose microchannels with a nonpermanent seal.<sup>31</sup> Some of the methods used to join dissimilar materials include double-stick tapes, epoxies, or simple gaskets. Unfortunately, upon prolonged exposure to aqueous environments, tape adhesive delaminates and can produce leaks at the joints of the microchannels. Epoxies promise a permanent bond between components, but the occurrence of flow channel occlusion during epoxy application, component assembly, and resin curing is likely as the excess of epoxy is squeezed from between the two surfaces to be joined.<sup>24</sup>

The ideal fabrication technology would take advantage of the multilayer construction concept used by polymer-based techniques, and it would overcome the sealing problems, following the silicon technologies approach. Some other characteristics, such as realistic cost without the need of special fabrication

conditions (clean rooms), would be of great interest in order to achieve mass production.

The low-temperature co-fired ceramics (LTCC) technology meets all these requirements showing unique capabilities to conjugate the most important features demanded by analytical microsystems designers: easy construction of complex three-dimensional structures by means of a multilayer method, monolithic integration of system components, and rapid prototyping at low cost.

Thus, a great variety of structures aimed at different analytical purposes can be easily constructed. Moreover, due to the ceramic layers characteristics, a compact and easy integration between fluidic, mechanical, and electrical components can be achieved. It also allows, in a simple way, the integration of multiple analytical paths in a single device without having structural problems related to the lack of sealing between layers or components.<sup>32</sup>

Recently, and as a proof of the synergic effect of these characteristics, this technology has been applied to the integration of mechanical and electrical components in tiny devices to obtain the so-called microelectromechanical systems.<sup>33</sup> These devices can range in size from a few micrometers to millimeters; they have the ability to sense, control, and actuate on the microscale and generate effects on the macroscale. Since the ceramic tape and all passive elements that may be embedded in it can be fired at the same time, they are said to be co-fireable. In addition to the possibility of creating complex three-dimensional structures, LTCC devices, once fired, are thermally stable compared to silicon devices, which generally work best at or near room temperature, 22 °C. Moreover, LTCC devices have been shown to work at temperatures exceeding 150 °C.<sup>34</sup> Another important advantage of the LTCC systems is that the devices are self-packaged; thus, there is no need to mount the completed device onto a substrate. Furthermore, due to the basic material of the ceramic, aluminum borosilicate, electroosmotic flows, similar to that of fused-silica capillaries, can be achieved.<sup>35</sup>

In this article, and as a first demonstration of the LTCC technology potential in the development of analytical microsystems, we propose and describe a general procedure for the fabrication of microfluidic structures that monolithically integrate potentiometric detectors based on solvent polymeric ion-selective electrodes. The miniaturized device also includes the reference electrode.

Plenty of work has already been done in the integration of these kinds of detectors in microfluidic manifolds constructed with different materials such as PDMS and silicon.<sup>15,20,36</sup> Tantra and Manz,<sup>37</sup> for example, developed an integrated potentiometric detector to be used in chip-based flow cells. When a potentiometric detector is used, since a reference electrode is needed as well,

(21) Puyol, M.; del Valle, M.; Garcés, I.; Villuendas, F.; Domínguez, C.; Alonso, J. *Anal. Chem.* **1999**, *71*, 5037–5044.

(22) Lai, S. Y.; Cao, X.; Lee, L. J. *Anal. Chem.* **2004**, *76*, 1175–1183.

(23) Unger, M. A.; Chou, H. P.; Thorsen, T.; Scherer, A.; Quake, S. R. *Science* **2000**, *288*, 113–116.

(24) Leatzow, D. M.; Dodson, J. M.; Golden, J. P.; Ligler, F. S. *Biosens. Bioelectron.* **2002**, *17*, 105–110.

(25) Wang, H. Y.; Foote, R. S.; Jacobson, S. C.; Schneibel, J. H.; Ramsey, J. M. *Sens. Actuators, B: Chem.* **1997**, *45*, 199–207.

(26) Becker, H.; Locascio, L. E. *Talanta* **2002**, *56*, 267, 287.

(27) Martynova, L.; Locascio, L.; Gaitan, M.; Kramer, G.; Christensen, R.; MacCrehan, W. *Anal. Chem.* **1997**, *69*, 4783–4789.

(28) McDonald, J. C.; Whitesides, G. M. *Acc. Chem. Res.* **2002**, *35*, 491–499.

(29) Wu, H. K.; Odom, T. W.; Chiu, D. T.; Whitesides, G. M. *J. Am. Chem. Soc.* **2003**, *125*, 554–559.

(30) Romanato, F.; Tormen, M.; Businaro, L.; Vaccari, L.; Stomeo, T.; Passaseo, A.; Di Fabrizio, E. *Microelectron. Eng.* **2004**, *73–74*, 870–875.

(31) Wang, J.; Pumera, M.; Chatrathi, M. P.; Escarpa, A.; Konrad, R.; Griebel, A.; Dörner, W.; Löwe, H. *Electrophoresis* **2002**, *23*, 596–601.

(32) Gongora-Rubio, M. R.; Espinoza-Vallejos, P.; Sola-Laguna, L.; Santiago-Aviles, J. J. *Sens. Actuators, A: Phys.* **2001**, *89*, 222–241.

(33) Gongora-Rubio, M.; Sola-Laguna, L. M.; Moffett, P. J.; Santiago-Aviles, J. J. *Sens. Actuators, A: Phys.* **1999**, *73*, 215–221.

(34) Bau, H. H.; Anathasuresh, S. G. K.; Santiago-Aviles, J. J.; Zhong, J.; Kim, M.; Yi, M.; Espinoza-Vallejos, P.; Sola-Laguna, L. In *Micro-Electro-Mechanical Systems (DSC–Vol. 66)*, 1998, International Mechanical Engineering Conference and Exposition; 1998; pp 491–498.

(35) Henry, C. S.; Zhong, M.; Lunte, S. M.; Kim, M.; Bau, H.; Santiago, J. J. *Anal. Commun.* **1999**, *36*, 305–307.

(36) Wang, J.; Pumera, M.; Chatrathi, M. P.; Rodríguez, A.; Spillman, S.; Martin, R. S.; Lunte, S. M. *Electroanalysis* **2002**, *14*, 1251–1255.

(37) Tantra, R.; Manz, A. *Anal. Chem.* **2000**, *72*, 2875–2878.

the integration and miniaturization of the whole instrumental setup becomes a great challenge. Some authors have presented different strategies in order to miniaturize the reference electrodes. Most of them are based on Ag/AgCl electrodes. However, the main problem found is the difficulty of isolating the reference solution from the sample one. To avoid interfering effects of the sample components or changes in the electrolyte composition of the reference semicell, which can affect the reference electrode response stability, two main approaches have been used. The first one consists of the use of a salt bridge to connect the sample and the reference solutions. Technological problems related to the fabrication process prevented us from working with this option at microscale. Nevertheless, some devices have been proposed that use, i.e., a glass-fiber filter as diaphragm to provide electric contact between the internal reference solution and the sample.<sup>38</sup> The second option includes the use of a different hydrophilic polymer (i.e., acrylic gel type) filled with the reference electrolyte solutions to substitute the salt bridge. Normally, these devices work properly during short periods of time and have been used in disposable sensors.<sup>39–41</sup>

Yalcinkaya and Powner<sup>42</sup> constructed an Ag/AgCl/Cl<sup>−</sup>-coated silver strip reference electrode that did not need an internal solution. In microfluidic systems, these problems may be circumvented by integrating the reference electrode outside the main channel. Our work presents a Ag/AgCl reference electrode fabricated by screen-printing over the ceramic tape and placed in a auxiliary channel through which continuously flowed a 0.1 M KCl solution to provide a constant reference potential. This solution was mixed with the carrier solution flowing through the main channel downstream the ion-selective electrode, acting as a free-flowing free-diffusion liquid junction.<sup>43</sup> The interface between the sample solution and the reference electrolyte was reproducible and a stable and minimized liquid junction potential was obtained.

The LTCC technique provides a great versatility, enabling the integration of screen-printed conductor paths that can be used as either metallic electrodes or as conductor inner support for membrane electrodes, and the creation of cavities and other three-dimensional structures that facilitate the whole integration of the potentiometric measurement setup.

## EXPERIMENTAL SECTION

**Reagents and Instrumental Setup.** All reagents used, of analytical grade, were obtained from Fluka. Stock solutions were prepared in MilliQ water weekly and kept in refrigerator. Standards were prepared by dilution of the stock solutions.

The hybrid continuous flow system setup consisted of a peristaltic pump (Minipuls 3, Gilson), a six-port distribution valve (Hamilton MVP, Reno, NV), 1.02-mm-i.d. silicon tubing (Ismatec, Zurich, Germany) and 0.8-mm-i.d. Teflon tubing (Scharlab, S.L., Cambridge, England), and the microanalytical system proposed.

A potentiometer with acquisition and recording signal software (TMI, Barcelona, Spain) was used. Some potentiometric measurements were performed vs a double-junction reference electrode (DJRE; Orion model 900200).

**Membrane Preparation and Deposition.** Two polymeric membranes (selective to ammonium ion and to nitrate ion) were evaluated in the LTCC system. The composition of the ammonium membrane<sup>44</sup> consisted of 1 wt % nonactine (Fluka), 65.5 wt % bis-(1-butylpentyl) adipate (Fluka) and 33.5 wt % PVC (Fluka). The nitrate membrane<sup>45–47</sup> consisted of 6 wt % tridodecylammonium nitrate ( $[(C_{12}H_{25})_3(CH_3)N]^+NO_3^-$ ) (Fluka), 65 wt % tris(2-ethyl)-hexyl phosphate (Fluka), and 29 wt % PVC (Fluka). These two membranes were chosen due to their well-known potentiometric response, described elsewhere. The comparison of the obtained results with those found in the literature was helpful in order to test the feasibility of our new system. The membrane components were weighed out and dissolved in THF. The amount of THF used depended on the membrane deposition methodology used:

**(a) Deposition by Simulating a Screen-Printing Technique.** A 3-mL sample of THF was used to dissolve the membrane components. The mixing was left to evaporate until ~1 mL of THF remained. The cocktail viscosity was then high enough so that it could be placed over the connecting hole without leakage problems. Two cocktail drops were deposited on the conductor path and expanded with the help of a slide. The path had a 500- $\mu$ m-diameter hole to facilitate the contact between the deposited membrane and the liquid flowing through the inner channel.

**(b) Membrane Gluing.** A 4-mL sample of THF (0.05 mL/mg of PVC) was used to dissolve the membrane components. After that, the cocktail was introduced in a Teflon container covered with a filter paper. It was left there for 24 h, until the THF was completely evaporated. The membrane was then cut in circular shape (i.d. 7 mm) and glued by means of a mixture of PVC and THF, over the 4-mm-diameter hole, which had been mechanized in the conductor path. Through this hole, the membrane was in contact with the solution flowing through the inner channel.

**LTCC Device Construction.** The LTCC general fabrication procedure is summarized in Figure 1. Starting from the initial CAD drawing, the different tapes had to be individually mechanized, laminated by means of a thermocompression process and finally burnt out in a furnace.

In this case, low-temperature co-fired ceramics 951 tapes (thickness of 254  $\mu$ m) supplied by DuPont were used. The process of shrinkage, caused by the binder burnout, is for many ceramics products the most critical step in the general aim of obtaining fully controlled microstructures and the desired final shape and dimensions. An average shrinkage reported by DuPont is of ~12.3% in the (x, y) direction and of 15% in the z direction.<sup>48</sup> To compensate it, shrinkage must be taken into account when the design is being done. The ceramic layers were first generated in

(38) Mroz, A.; Borchardt, M.; Diekmann, C.; Cammann, K.; Knoll, M.; Dumschat, C. *Analyst* **1998**, *123*, 1373–1376.

(39) Ciobanu, M.; Wilburn, J.; Lowy, D. A. *Electroanalysis* **2004**, *16*, 1351–1358.

(40) Huang, I. Y.; Huan, R. S.; Lo, L. H. *Sens. Actuators, B: Chem.* **2003**, *94*, 53–64.

(41) Ciobanu, M.; Wilburn, J. P.; Buss, N. I.; Ditavong, P.; Lowy, D. A. *Electroanalysis* **2002**, *14*, 989–997.

(42) Yalcinkaya, F.; Powner, E. T. *Med. Eng. Phys.* **1997**, *19*, 299–301.

(43) Dohner, R. E.; Wegmann, D.; Morf, W. E.; Simon, W. *Anal. Chem.* **1986**, *58*, 2585–2589.

(44) Alegret, S.; Alonso, J.; Bartroli, J.; Martinez-Fabregas, E. *Analyst* **1989**, *114*, 1443–1447.

(45) Alegret, S.; Alonso, J.; Bartroli, J.; Paulis, J. M.; Lima, J. L. F. C.; Machado, A. A. S. C. *Anal. Chim. Acta* **1984**, *164*, 147–152.

(46) Alegret, S.; Alonso, J.; Bartroli, J.; Lima, J. L. F. C.; Machado, A. A. S. C.; Paulis, J. M. *Anal. Lett.* **1985**, *18*, 2291–2303.

(47) Knoll, M.; Cammann, K.; Dumschat, C.; Eshold, J.; Sundermeier, C. *Sens. Actuators, B: Chem.* **1994**, *21*, 71–76.

(48) [http://www.mcm.dupont.com/MCM/en\\_US/Products/greentape/greentape.html](http://www.mcm.dupont.com/MCM/en_US/Products/greentape/greentape.html); October 2005.



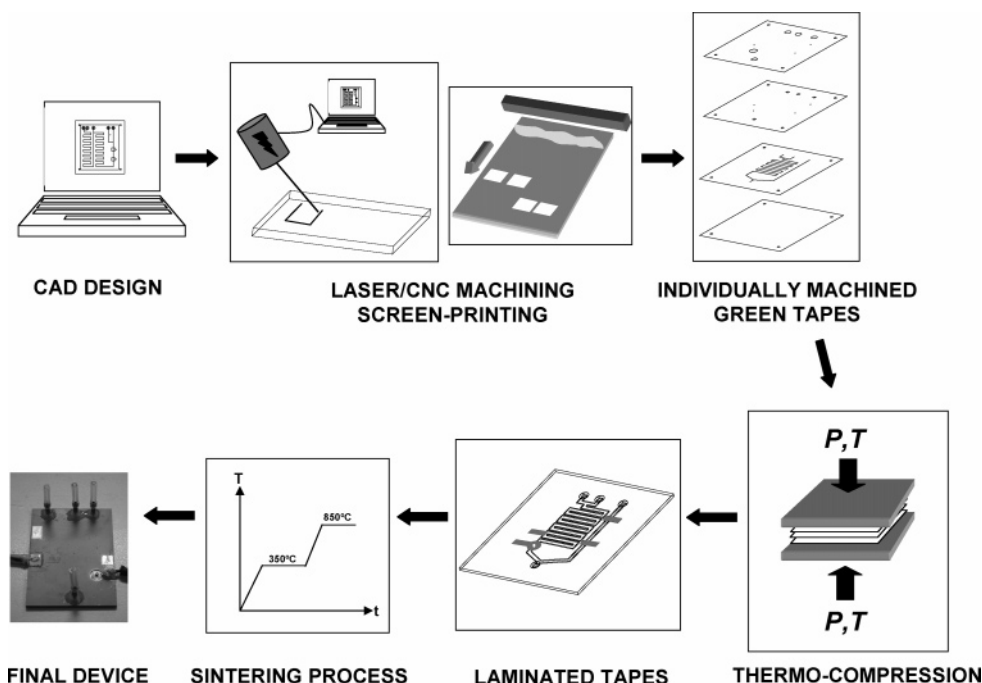


**Figure 1.** General fabrication procedure of a LTCC device.

a CAD program. A LKPF ProtoMat C100/HF (LKPF) milling machine was used to transfer the designed layers to the ceramic tapes. Mills and drill bits from 0.2- to 2.5-mm diameter were used. The size of the features that can be fabricated by means of the CNC machine, using these ceramics, is determined by the diameter of the tool, the thickness of the ceramic tapes, and the shrinkage caused by the firing step. Hence, the minimum channel dimensions that could be achieved after being sintering would be of  $\sim 0.17$ -mm width and  $\sim 0.21$ -mm depth. Smaller feature sizes, which could be needed for some other applications such as capillary electrophoresis, could be achieved by means of a laser machine.<sup>35</sup>

The CircuitCAM software based on Windows was used to adapt directly and easily the CAD designs to the CNC machine. Conductor screen-printed paths were deposited using a DEK 248 printer (Asflex Internacional).

The alignment of the different layers was achieved due to four placing holes in the corners of each layer. The lamination method used was thermocompression. A hydraulic press (Talleres Francisco Camps, S. A., Granollers, Spain) was especially fabricated for this purpose. It consisted of two  $250 \times 150$  mm heating plates, whose temperature was controlled by means of a probe and a resistance. The ceramic tapes that had previously been placed between the plates were heated at  $100^\circ\text{C}$  for a minute at 1000 psi. After that, the pressure was incremented until 3000–3500 psi, for 2–4 min.

Finally, the laminated device was burnt out in air atmosphere in a box furnace (Carbolite CBCWF11/23P16, Afora, Spain). The laminates were carefully ( $10^\circ\text{C}/\text{min}$ ) burnt out to  $350^\circ\text{C}$  during 30 min, followed by sintering at  $850^\circ\text{C}$  (also achieved at  $10^\circ\text{C}/\text{min}$ ) for 30 min. At  $600$ – $760^\circ\text{C}$ , depending on the glass composition, the glass softening takes place and the interpenetration of the alumina particles starts.

To test both proposed membrane deposition procedures, two slightly different ceramic devices were constructed in this work.

These differences are related to the membrane surface area in contact with the inner flowing solution, which is defined by the diameter of the hole where the membrane had to be deposited. When the membrane was deposited by screen-printing, a  $500\text{-}\mu\text{m}$ -diameter hole was drilled instead of the 4-mm-diameter hole, onto which the circular-shaped sensing membrane was glued. Except from this difference, their fabrication process, explained before, was the same for each of them. As an example, Figure 2A shows the component layers of the device where membrane was deposited by screen-printing. The design of the ceramic tapes was made one by one taking into account that their final overlap should result in the three-dimensional geometry desired. The overlapping of the layers (layer a the upper one and d the bottom one) resulted in the final LTCC device. The cavity where the membrane is deposited was mechanized in layer a; layer b contained the via that provided contact between the flowing solution and the membrane.

Three rectangular conductor paths ( $1 \times 0.5$  cm) (TC0307, Heraeus) were printed on the back of layer b (showed as dashed rectangles in Figure 2A). Once the ceramic layers were overlapped, these paths got in contact with the flowing solutions in the channels. Two of these conductor paths, placed before the reference and the indicator electrodes, were used as ground connections, with the aim of avoiding streaming potentials, typical electrical noise caused by the pump or the valve, which is pretty common in flow systems. The other conductor path was used as a reference electrode after surface modification by electrolysis. Layer b also shows some vias that were filled with conductor paste (TC0308, Heraeus) to provide electric contact between the inner conductor paths (on the back of layer b) and the device surface, onto which three more paths (TC0306, Heraeus) were printed in order to afford the connection with the external electronic setup used in signal measurements. The circular conductor path in layer a (TC0306, Heraeus) was used as inner conductor support for the ion-selective membrane. The difference

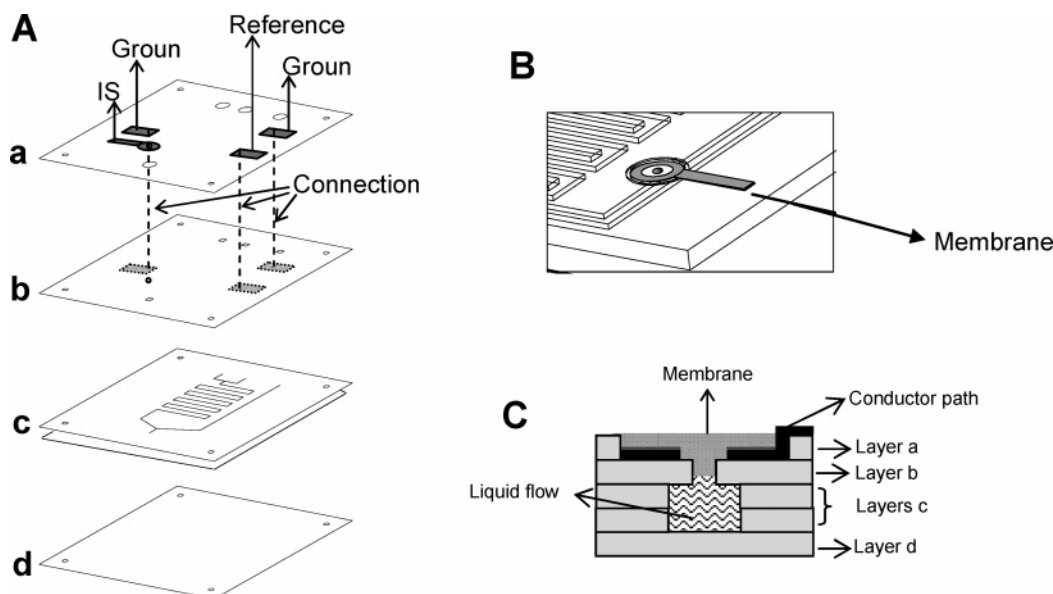


**Figure 2.** (A) Component layers: (a) upper layer (connections and cavity to enable membrane deposition); (b) intermediate layer (conductor path); (c) channels layer (width determined by the diameter of the tool and depth determined by the number of ceramic layers containing the mechanized channels, 2 in this application); (d) bottom layer. On the back of layer b, inner conductor paths (ground connections and reference electrode). (B) Detailed 3D view of the deposited membrane. (C) Schematic view of the cross section of the deposited membrane.

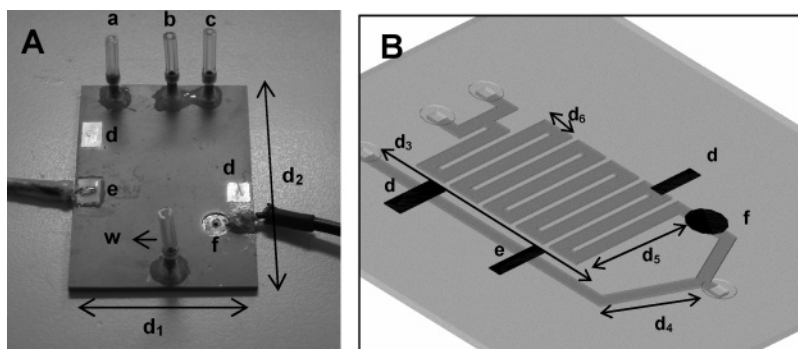


**Figure 3.** LTCC device pictures (screen-printing deposition). (A) (a)  $\text{Cl}^-$  solution inlet; (b) water/sample solution inlet; (c) carrier solution inlet; (d) ground connection; (e) reference electrode connection; (f) conductor path where the membrane is deposited. w, waste (flow outlet);  $d_1$ , 3.9 cm;  $d_2$ , 5.3 cm. (B) Inner architecture of the LTCC structure:  $d_3$ , 3.9 cm;  $d_4$ , 1.4 cm;  $d_5$ , 18.4 mm;  $d_6$ , 2.7 mm.

between the Heraeus screen-printing pastes (all of them containing pure Ag as a conductor) is the function they are optimized for. Thus, TC0306 is a surface conductor, TC0307 is a routing conductor, and TC0308 is a dense via fill. Figure 2B shows a schematic three-dimensional view of the layers once overlapped, especially focusing on the deposited membrane. Figure 2C shows a more detailed view of the cross section of the deposited ion-selective membrane. It can be seen that the membrane is simultaneously in contact with the conductor path and with the flowing solution due to the hole drilled in layers a and b. The fluidic channels were mechanized in layer c. A free space was left between the drilled hole and the printed conductor path to prevent the appearance of undesired mixed potentials. After the sintering step, the sensing membrane would be deposited onto it by means of the before mentioned techniques.

Figure 3A shows a picture of the device where the membrane was deposited by screen-printing. A three-dimensional drawing can be seen in Figure 3B. Some details about the channel sizes are given. In this application, the channels were mechanized by means of a 1.3-mm-diameter contour router in two ceramic layers (layer c). This means that, before the firing step, the channel width

was 1.3 mm and their depth was  $508\ \mu\text{m}$  ( $2 \times 254\ \mu\text{m}$  each ceramic layer). Due to the ceramic shrinkage, after the firing step (12.3% in the  $x$ - $y$  and 15% in the  $z$  axis), the channel dimensions were  $\sim 1.1$ -mm width and  $\sim 431\text{-}\mu\text{m}$  depth. Although smaller sizes could have been achieved, it was not necessary for our present purposes.

The anodization of the Ag conductor path (indicated as e in Figure 3), to cover it with a AgCl layer, was achieved by applying a voltage of 0.8 V for 20 min in the presence of a 0.2 M KCl solution.

## RESULTS

The aim of this paper is to show the viability of the LTCC technology as an alternative to the conventional microfabrication techniques for the construction of analytical microsystems, taking advantage of the possibility of constructing three-dimensional structures that greatly facilitate the incorporation of different stages of the analytical process.

In this way, a general procedure to construct continuous flow analytical microsystems integrating potentiometric detection based on solvent polymeric ISE has been evaluated.

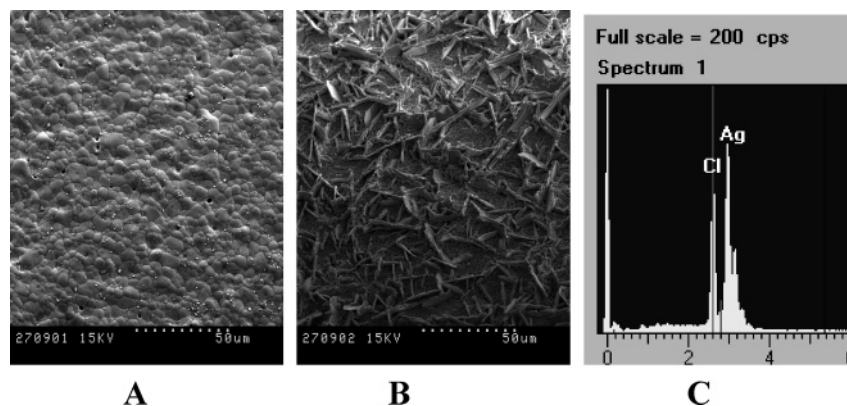


**Figure 4.** SEM pictures of the Ag conductive path: (A) before the anodization; (B) after the anodization; (C) X-ray photoelectron spectroscopy showing the formation of AgCl.

To prove its general usefulness, two different ion-selective membranes have been evaluated. The procedure used to determine the response characteristics of the LTCC device was the same for both tested membranes. Initially, the influence of experimental hydrodynamic and chemical parameters such as flow rate, injection volume, and buffer concentration on the microsystem response was evaluated. Once the optimization process was performed, analytical features were determined through calibration experiments.

The results obtained by the two integrated potentiometric liquid ion-exchanger selective membranes have been similar to those obtained by conventional electrodes.

**Flow Microsystem Manifold.** The general view of the flow system manifold can be seen in Figure 3. Channel a is the auxiliary channel through which a 0.1 M KCl solution flows constantly in order to keep the reference potential stable. The sample (b) (nitrate or ammonium standards) and the carrier (c) solution channels mix together upstream the ion-selective electrode (showed as (f) in Figures 3). This helps to adjust the pH and the ionic strength of the samples to be analyzed. Finally, both the KCl flowing solution and the main one, mix together downstream the ion-selective electrode, to provide electric contact between the reference and the ISE, before they flow through the waste outlet.

**Reference Electrode.** Previous to its integration in the LTCC system and to test the stability of the signal provided by the screen-printed reference electrode, some experiments were performed in batch. For this purpose, some conductor paths were screen-printed onto small LTCC tapes. After the sintering step, a cable was soldered onto a half of the Ag conductor path and AgCl was deposited on the other half of it, as explained before. The experiment was performed in dark conditions. Figure 4 shows SEM pictures of the Ag path before (Figure 4A) and after (Figure 4B) the anodization step. After the electrolysis, an X-ray photoelectron spectroscopy of the screen-printed path was performed (Figure 4C). It was observed that AgCl had been deposited in the whole surface. The reference electrode potential was measured continuously for 2 h in a 0.1 M KCl stirred solution versus a DJRE. The drift obtained was 0.027 mV/min. The reference electrode was then evaluated once it had been integrated in the LTCC system. During the experiments, a 0.1 M KCl solution flowed constantly through the auxiliary channel where the reference electrode (working as indicator in this case) was placed. The

potential was recorded versus a DJRE for 2 h. The drift obtained (0.042 mV/min) was slightly higher than in batch conditions. However, and as can be seen in later experiments, the results obtained by the reference electrode showed its suitability to be integrated in the LTCC microsystems.

**Ammonium Microsystem.** For the ammonium ion LTCC microsystem, TRIS (pH 7.4 adjusted with HCl) and water solutions were mixed inside the microfluidic device through a confluence point situated upstream the ion-selective membrane. The resulting solution was used to define the baseline signal. To get a constant reference signal and to avoid interfering effects on the ion-selective membrane response, the reference electrode was placed in an auxiliary channel (see Figure 3). A 0.1 M KCl solution flowed through this channel and it was mixed, downstream the indicator electrode, with the main channel. When an ammonium standard was injected in the water solution channel, a typical FIA peak was obtained.

For both device versions, the experimental parameters studied were as follows: flow rate (ranging between 0.4 and 2.00 mL/min), injection volume (from 50 to 450  $\mu$ L), and carrier (TRIS) concentration (from 0.005 to 0.05 M). The optimized values for the screen-printing membrane deposited device, chosen as a compromise situation between the maximum possible signal and the better sampling rate, were as follows: flow rate 1.15 mL/min, injection volume 450  $\mu$ L, and [TRIS] = 0.005 M.

Analytical features of the proposed microsystem were determined from calibration experiments. The calibration equation obtained ( $n = 5$  and 95% confidence) was  $E = 2(\pm 5) + 46(\pm 3) \log[\text{NH}_4^+]$ , with  $r^2 > 0.995$ . The linear working range was found to be 2–50 ppm. Higher ammonium concentrations were not tested. The detection limit found, according to IUPAC,<sup>49</sup> was  $0.48 \pm 0.04$  ppm ( $n = 7$ ). Repetitivity studies were performed by successive injections of a 0.5 ppm  $\text{NH}_4^+$  standard solution. The average peak height obtained was  $12 \pm 1$  mV and RSD = 11.08% ( $n = 7$ , 95% confidence). These results showed the robustness of the whole experimental setup, even when concentrations around the detection limit were used.

To test the performance of the miniaturized reference electrode integrated in the microfluidic structure, the ammonium-selective membrane response was evaluated also versus an external DJRE.

(49) *CRC Handbook of Ion-Selective Electrodes*; CRC Press: Boca Raton, FL, 1990.

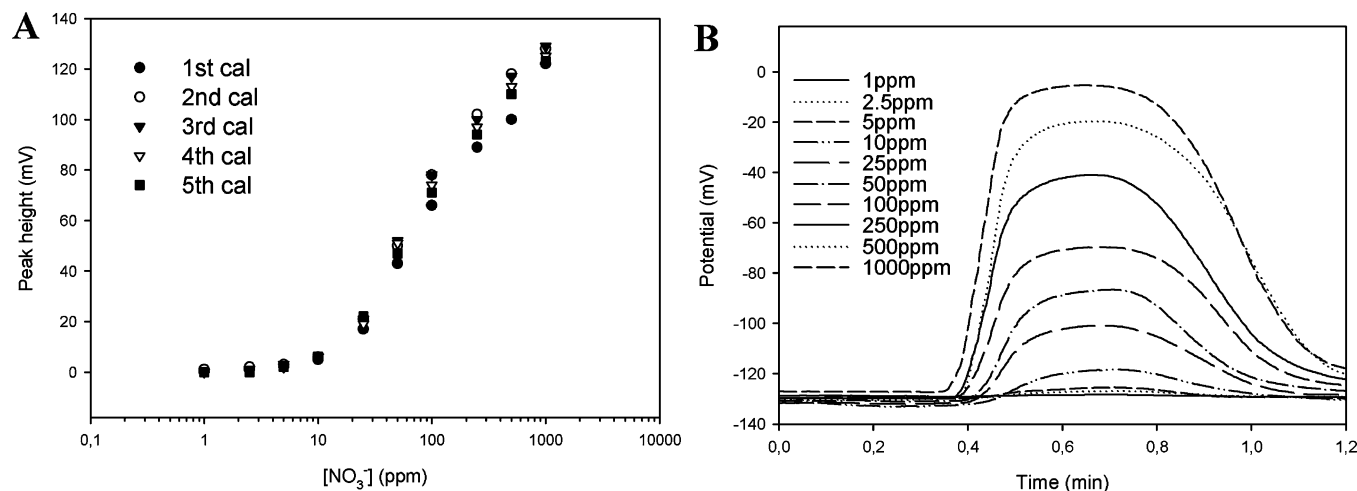


**Figure 5.** (A) Calibration plots and (B) FIA peaks. Both obtained using the integrated reference electrode.

**Table 1. Analytical Parameters of the Comparison of the Results Obtained with the Ammonium Microsystem and Both Reference Electrodes**

analytical parameters	integrated reference electrode	DJRE
calibration plot	$E = 2(\pm 5) + 46(\pm 3) \log[\text{NH}_4^+]$ ; $r^2 > 0.995$ ( $n = 5$ , 95%)	$E = 5(\pm 6) + 44(\pm 4) \log[\text{NH}_4^+]$ ; $r^2 > 0.995$ ( $n = 3$ , 95%)
linear working range	2–50 ppm	2–50 ppm
LOD <sup>18</sup>	$0.48 \pm 0.04$ ppm ( $n = 7$ )	$0.47 \pm 0.04$ ppm ( $n = 3$ )
repetitivity RSD (%) (0.5 ppm)	11.08% ( $n = 7$ , 95%)	8.33% ( $n = 7$ , 95%)

Results obtained, as well as those previously obtained by the miniaturized reference electrode, are summarized in Table 1. As can be seen, no significant differences could be observed for any of the analytical parameters evaluated, demonstrating the usefulness of the integrated reference electrode.

The evaluation of the second deposition procedure (the gluing method) was also performed. Both LTCC devices (the screen-printing and the gluing one) were compared under the same experimental conditions. It was observed that the glued membrane response was worse than the screen-printed one, previously described. Only when a flow rate half the optimized one was used, increasing the contact time between sample and membrane, similar calibration curves were obtained for both devices. This phenomenon can be related to the higher thickness of the glued membrane. Additionally, the larger membrane surface could be more easily deformed at high flow rates, restricting the robustness of the microanalytical system. Finally, the screen-printing method for the membrane deposition was chosen because it was simpler, faster, and easier to be automated.

**Nitrate Microsystem.** To test the behavior of other polymeric membranes when integrated in the LTCC device, a nitrate membrane was prepared, deposited by means of the screen-printing technique, and evaluated. The optimization of the experimental parameters was carried out in the same way as those for the ammonium membrane. The experimental parameters studied were as follows: flow rate (ranging between 0.69 and 1.87 mL/min), injection volume (from 150 to 1720  $\mu\text{L}$ ), and carrier ( $\text{K}_2\text{SO}_4$ ) concentration (from 0.025 to 0.5 M) adjusted with  $\text{H}_2\text{SO}_4$  at two pHs (2.4 and 5.5). The optimized values, chosen as a compromise situation between the maximum possible signal and the better sampling rate, were as follows: flow rate

1.15 mL/min, injection volume 680  $\mu\text{L}$ , and  $[\text{K}_2\text{SO}_4] = 0.1$  M (pH 2.4). The nitrate microsystem was calibrated with the optimized experimental conditions. The response parameters were (for  $n = 5$  and 95% confidence) as follows:  $E = -57(\pm 3) + 63(\pm 3) \log[\text{NO}_3^-]$ ;  $r^2 > 0.993$ . The linear working range was established between 10 and 500 ppm. LOD =  $7.9 \pm 0.2$  ppm. Figure 5A shows the calibration plots obtained, as well as the FIA peaks (Figure 5B).

To test the reproducibility of the screen-printing deposition methodology, three nitrate-selective membranes were deposited in the course of three weeks and different calibrations of the microsystem were carried out with each of them. A single-factor ANOVA was performed with the slope values of calibration curves obtained with the three deposited membranes, and no significant differences could be observed ( $F_{\text{exp}} = 3.93 < F_{\text{tab}} = 4.74$ ). This results confirm that the established ion-selective membrane deposition methodology was reproducible.

The lifetime of the membranes, once integrated in the constructed devices, was not evaluated for long periods of time. However, they did not show loss of their analytical properties during a month of continuous testing. Taking into account the information found in the literature regarding these cocktail membranes when working in conventional flow systems, it can be assumed that the working period can exceed six months, depending obviously on the kind of samples to be analyzed.

## CONCLUSIONS

The LTCC technology enables the rapid construction of three-dimensional structures and, moreover, the easy integration of different unitary operations of the analytical process. In this work, a general procedure for the integration of ISEs, based on



polymeric membranes as detectors, has been proposed and evaluated. Two different ion-selective membranes have been easily integrated by means of two different membrane deposition methodologies. Although both of them showed good results, the screen-printing technique turned out to be simpler, faster, and easier to be automated. The obtained results were comparable to those provided by the same ISE in conventional continuous flow systems. Additionally, an inner Ag/AgCl reference electrode has also been integrated in the LTCC mesofluidic manifold and compared with an external double-junction reference electrode. Results provided by both systems were identical.

#### **ACKNOWLEDGMENT**

N.I.-G. is thankful for an FPI grant from the Universitat Autònoma de Barcelona. Financial support received from Generalitat de Catalunya (ACI2003-40/AIRE2003-8) and Spanish Education Ministry (PHB2004-0105-PC, DPI2003-09735-C02-01 and FIT310200-2004-38) are also acknowledged.

Received for review November 9, 2005. Accepted February 28, 2006.

AC051994K